

Effect of Iron and Organophosphorus Flame Inhibitors on the Heat Release Rate in Hydrogen/Oxygen Flames at Low Pressure

Vladimir M. Shvartsberg,* Tatyana A. Bolshova, and Oleg P. Korobeinichev

Institute of Chemical Kinetics and Combustion, Institutskaya 3, Novosibirsk 630090, Russia

Received November 3, 2010. Revised Manuscript Received December 15, 2010

The influence of chemically reactive inhibitors of hydrocarbon flames, such as atomic iron and trimethyl phosphate, on the heat release rate in a laminar premixed lean ($\phi = 0.37$) $\text{H}_2/\text{O}_2/\text{Ar}$ flame at a pressure of 3 kPa is studied by numerical modeling. It is established that the addition of atomic iron to the flame results in additional heat release because of reactions involving iron-containing species and increases the flame temperature to the equilibrium value. In the Fe-doped flame, the additional heat is found to be released at a higher temperature than the heat from hydrogen oxidation. Unlike in the iron-doped flame, in the flame doped with trimethyl phosphate, the additional heat is released in the same flame region as the heat from hydrogen oxidation. The dopant increases or does not increase the rate of the chain-branching reaction, depending upon the flame region where the additional heat is released. This determines the nature of the effect of the dopant on the flame (inhibition or promotion). The reaction of iron hydroxide formation $\text{FeO} + \text{H}_2\text{O} = \text{Fe}(\text{OH})_2$ is shown to make the main contribution to the additional heat release in the Fe-doped flame, whereas in the flame doped with trimethyl phosphate, the additional heat is almost entirely released in the reaction $\text{H} + \text{PO}_2 + \text{M} = \text{HOPO} + \text{M}$.

1. Introduction

Some chemically active inhibitors of hydrocarbon flames are known to promote hydrogen/oxygen flames. The mechanism of flame inhibition, as a rule, involves processes of catalytic recombination of active flame species, whereas the promotion mechanisms are diverse for different compounds and flames. The mechanism of promotion of $\text{H}_2/\text{O}_2/\text{Ar}$ flames by organophosphorus compounds (OPCs) at a pressure of about 50 Torr is one of the most thoroughly investigated.^{1–5} The action of OPCs as promoters was established experimentally from changes in the thermal and chemical structure of the flame^{1,2} and by modeling from an increase in the flame speed with increasing dopant concentration in the unburnt gases.³ Later, the promoting action of OPCs was explained in detail.⁵

Sulfur oxides are also inhibitors capable of increasing the speed of H_2/O_2 flames. A number of mechanisms for the action of sulfur oxides on flames have been proposed,^{6,7} but the reactions of catalytic recombination are similar to those of phosphorus compounds. However, in the development of these mechanisms, emphasis was placed on the ecological aspects of sulfur combustion, i.e., minimization of SO_x emission. This is explained by the absence of prospects for the application of

sulfur-containing compounds as flame inhibitors and fire suppressants because of their low effectiveness. Despite this, a high activity of SO_2 as a promoter of a low-pressure (47 Torr) premixed $\text{H}_2/\text{O}_2/\text{Ar}$ flame has been demonstrated⁸ by modeling the flame speed as a function of SO_2 loading. According to ref 8, the promotion effectiveness of SO_2 is nearly the same as that of trimethyl phosphate (TMP).

Iron pentacarbonyl [$\text{Fe}(\text{CO})_5$] and other iron-containing compounds are known to be effective inhibitors of hydrocarbon and hydrogen flame at atmospheric pressure.^{9–14} Nevertheless, $\text{Fe}(\text{CO})_5$ is able to accelerate the process of combustion and autoignition. Although the mechanism of action of $\text{Fe}(\text{CO})_5$ on flames is based on recombination of chain carriers catalyzed by iron-containing species (ICS), the mechanism underlying the promoting action of $\text{Fe}(\text{CO})_5$ differs fundamentally from the promotion mechanisms of phosphorus and sulfur. Two cases of promoting effects of $\text{Fe}(\text{CO})_5$ are described in the literature: an increase in the burning velocity of a $\text{CO}/\text{N}_2\text{O}$ flame¹⁵ and a decrease in the autoignition delay of a H_2/air mixture.

It has been demonstrated¹⁵ that the speed of propagation of a $\text{CO}/\text{N}_2\text{O}$ flame (unbranched chain process) is increased by the addition of small amounts of $\text{Fe}(\text{CO})_5$. It has been suggested¹⁵ that the acceleration of CO oxidation occurs by

*To whom correspondence should be addressed. Telephone: +7-(383)-333-33-46. Fax: +7-(383)-330-73-50. E-mail: vshvarts@kinetics.nsc.ru.

(1) Korobeinichev, O. P.; Chernov, A. A.; Shvartsberg, V. M. *Prepr. Pap.—Am. Chem. Soc., Div. Fuel Chem.* **1994**, 39 (1), 193–197.

(2) Korobeinichev, O. P.; Shvartsberg, V. M.; Chernov, A. A.; Mokrushin, V. V. *Proc. Combust. Inst.* **1996**, 26, 1035–1042.

(3) Korobeinichev, O. P.; Ilyin, S. B.; Bolshova, T. A.; Shvartsberg, V. M.; Chernov, A. A. *Combust. Flame* **2000**, 121 (4), 593–609.

(4) Korobeinichev, O. P.; Bolshova, T. A.; Shvartsberg, V. M.; Chernov, A. A. *Combust. Flame* **2001**, 125 (1–2), 744–751.

(5) Bolshova, T. A.; Korobeinichev, O. P. *Combust., Explos. Shock Waves (Engl. Transl.)* **2006**, 42 (5), 493–502.

(6) Zachariah, M. R.; Smith, O. I. *Combust. Flame* **1987**, 69 (2), 125–139.

(7) The Leeds methane oxidation mechanism (available at <http://garfield.chem.elte.hu/Combustion/methane.htm>).

(8) Korobeinichev, O. P.; Panfilov, V. N.; Shvartsberg, V. M.; Bolshova, T. A. *Combust., Explos. Shock Waves (Engl. Transl.)* **2010**, 46 (2), 140–148.

(9) Lask, G.; Wagner, H. G. *Proc. Combust. Inst.* **1962**, 26, 432–438.

(10) Miller, D. R.; Evers, R. L.; Skinner, G. B. *Combust. Flame* **1963**, 7, 137–142.

(11) Vanpee, M.; Shirodkar, P. *Proc. Combust. Inst.* **1979**, 18, 787–793.

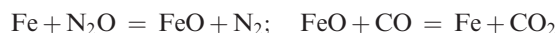
(12) Reinelt, D.; Linteris, G. T. *Proc. Combust. Inst.* **1996**, 26, 1421–1428.

(13) Rumminger, M. D.; Reinelt, D.; Babushok, V.; Linteris, G. T. *Combust. Flame* **1999**, 116, 207–219.

(14) Shvartsberg, V. M.; Bolshova, T. A.; Korobeinichev, O. P. *Energy Fuels* **2010**, 24 (3), 1552–1558.

(15) Linteris, G. T.; Rumminger, M. D.; Babushok, V. I. *Combust. Flame* **2000**, 122, 58–75.

catalytic oxygen atom transfer from N_2O to CO.



FeO and FeOH also transfer an oxygen atom from N_2O to CO. The dopant promotes combustion because the catalytic pathway of CO oxidation is faster than the direct reaction of $\text{CO} + \text{N}_2\text{O}$. The promotion effectiveness decreases with the addition of hydrogen to the flame because of the formation of OH, which effectively oxidizes carbon monoxide: $\text{CO} + \text{OH} = \text{CO}_2 + \text{H}$. As the H_2 concentration in the unburnt gases increases, the catalytic oxidation loses its significance in this system.

Autoignition of lean and stoichiometric H_2/air mixtures in the presence of various iron-containing compounds [$\text{Fe}(\text{CO})_5$, Fe, FeO , and FeOH] at 1000 K has been studied by numerical modeling.¹⁶ At a dopants concentration less than 150 ppm, a decrease in the ignition delay (by a factor of 2–3) was observed; i.e., promotion occurred. The promotion effectiveness is the highest for FeO additives and the lowest for $\text{Fe}(\text{CO})_5$. It is noteworthy that, at a level above 1500 ppm, the dopants inhibit autoignition (increase the ignition delay). It has been demonstrated¹⁶ that promotion is due to the formation of H, O, and OH in the reactions of Fe with H_2 and O_2 in an early stage of the ignition process.

Staupe et al.¹⁷ measured temperature profiles in a laminar adiabatic premixed $\text{H}_2/\text{O}_2/\text{Ar}$ flame ($\phi = 0.37$) without additives and with iron pentacarbonyl at a pressure of 3 kPa. The addition of $\text{Fe}(\text{CO})_5$ was shown to increase the flame temperature throughout the combustion zone. It was suggested¹⁷ that the dopant increased the flame speed at low pressure, i.e., promoted the flame.

The goal of the present work was to verify this hypothesis by comparing the effect of atomic iron and TMP on the heat release rate and chain-branching rate in a low-pressure lean $\text{H}_2/\text{O}_2/\text{Ar}$ flame. It was also of interest to determine the influence of the choice of the kinetic model for hydrogen oxidation on the nature and effectiveness of the dopant action on the flame.

2. Modeling

The speed and structure of a freely propagating $\text{H}_2/\text{O}_2/\text{Ar}$ (0.52924:0.26462:0.20614) flame doped with atomic iron and TMP at $P = 3$ kPa (≈ 22.5 Torr) was simulated using the Premix and Chemkin codes.^{18,19} For modeling, three modern mechanisms for hydrogen oxidation were chosen.^{20–22} The chosen models were validated by comparing modeled and measured concentration profiles of H, O, and OH in a burner-stabilized stoichiometric $\text{H}_2/\text{O}_2/\text{Ar}$ flame at 47 Torr²³ (panels a–c of Figure 1). Modeling of the burner-stabilized flames was performed using temperature

(16) Linteris, G. T.; Babushok, V. I. *Proc. Combust. Inst.* **2009**, 32 (2), 2535–2542.

(17) Staupe, S.; Hecht, C.; Wlokas, I.; Schulz, C.; Atakan, B. *Z. Phys. Chem.* **2009**, 223, 639–649.

(18) Kee, R. J.; Grcar, J. F.; Smooke, M. D.; Miller, J. A. A program for modeling steady, laminar, one-dimensional premixed flames. *Report SAND85-8240*; Sandia National Laboratories: Albuquerque, NM, 1985.

(19) Kee, R. J.; Rupley, F. M.; Miller, J. A. Chemkin II: A Fortran chemical kinetics package for the analysis of gas-phase chemical kinetics. *Report SAND89-8009*; Sandia National Laboratories: Albuquerque, NM, 1989.

(20) Conaire, M. O.; Curran, H. J.; Simmie, J. M.; Pitz, W. J.; Westbrook, C. K. *Int. J. Chem. Kinet.* **2004**, 36 (11), 603–622.

(21) Li, J.; Zhao, Zh.; Kazakov, A.; Dryer, F. L. *Int. J. Chem. Kinet.* **2004**, 36 (10), 566–575.

(22) Konnov, A. A. *Combust. Flame* **2008**, 152, 507–528.

(23) Korobeinichev, O. P.; Shvartsberg, V. M.; Chernov, A. A. *Combust. Flame* **1999**, 118, 727–732.

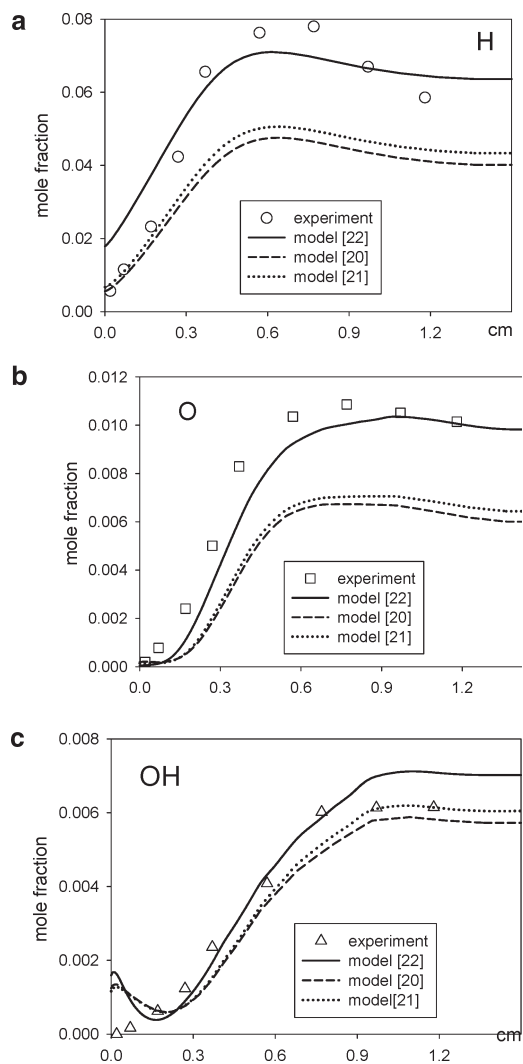


Figure 1. Measured²³ (symbols) and simulated (curves) spatial variations of the mole fraction of (a) H atoms, (b) O atoms, and (c) OH radicals in a $\text{H}_2/\text{O}_2/\text{Ar}$ (0.26:0.13:0.61) flame stabilized on a flat burner at 47 Torr and 368 K.

profiles that were measured experimentally (with microthermocouples) rather than solving the energy equation.

Panels a and b of Figure 1 show that Konnov's model²² is the best in predicting spatial variations of H and O atoms, whereas Dryer's model²¹ is more accurate in predicting OH concentrations (Figure 1c). Taking into account the $\pm 50\%$ confidence range of the experimental results, it can be concluded that all models^{20–22} adequately predict the concentration profiles of chain carriers in the low-pressure flame. Therefore, we decided to use all of these models for H_2 oxidation in the subsequent simulations.

According to ref 24, $\text{Fe}(\text{CO})_5$ readily decomposes under heating to give atomic iron; therefore, we used Fe as a dopant to the flame to avoid the effect of carbon monoxide on the stoichiometry of the flame. Thus, all reactions involving carbon-containing species were eliminated from the mechanism of flame inhibition by iron pentacarbonyl.²⁴

In addition to the above-mentioned mechanisms for H_2 oxidation, a model for flame inhibition (promotion) by TMP³ was also used in the simulation of the structure of TMP-doped flames. This model includes reactions of catalytic recombination involving phosphorus oxides and acids. The mechanism was applied for simulation of the structure low-pressure $\text{H}_2/\text{O}_2/\text{Ar}$ and

(24) Rumminger, M. D.; Reinelt, D.; Babushok, V. I.; Linteris, G. T. *Combust. Flame* **1999**, 116, 207–219.

CH₄/O₂/Ar flames doped with organophosphorus compounds.^{3,4} Bolshova and Korobeinichev⁵ explained the promotion effect of organophosphorus compounds on hydrogen flames at 50 Torr based on the model.³

In the modeling of freely propagating adiabatic flames, the energy conservation equation was solved and windward differencing was used. The grid was refined to GRAD = 0.1 and CURV < 0.2, with thermal and multicomponent diffusion taken into account. The computational grid domain was from –5 to 20 cm, and its further increase did not influence the flame speed and structure.

Spatial variations of the heat release rate and chain-branching rate in the flame were calculated using the KINALC code,²⁵ a postprocessor of the output files of the PREMIX code. Because the reaction mechanism used in the calculations contained only irreversible reactions, the original mechanisms^{20–22,24,3} were first converted to an irreversible form by the MECHMOD code.²⁶ We note that, although the heat release and net reaction rates via particular reactions were calculated by irreversible reactions, below, the heat release is given as a net reaction rate for the reversible reaction.

3. Results and Discussion

3.1. Effect of Iron on the Heat Release Rate. Spatial variations of the temperature in the undoped adiabatic flame were simulated using models from refs 20–22 (Figure 2a). Temperature profiles obtained for different models differed considerably in final values (temperature at the right boundary of the computational grid) and shape. These differences were also reflected in the temperature profiles for the Fe-doped flames (Figure 2b). The shape of the profile simulated using Curran's model²⁰ is quite usual, whereas the profiles obtained for the other models from refs 21 and 22 (especially Konnov's model²²) have a pronounced two-zone structure. The final temperature for the doped flame was calculated to be 2390 ± 2 K (Table 1) and was almost the same as the equilibrium temperature for the given system under the given conditions. The addition of 0.1% (by volume) of atomic iron was shown to have a negligible effect on the equilibrium temperature of the flame. The data presented in panels a and b of Figure 2 suggest that a small additive of iron to a lean H₂/O₂/Ar flame increases the final flame temperature.

Flame speed calculations using various models for H₂ oxidation did not provide a clear answer to the question of whether iron additives promote or inhibit lean low-pressure H₂/O₂/Ar flames. Burning velocities of the undoped and Fe-doped (1000 ppm) flame simulated using mechanisms from refs 20–22 are given in Table 1. Curran's model²⁰ predicts an about 1% increase in the flame speed, whereas Dryer's²¹ and Konnov's²² models predict an about 2.6–2.7% decrease in the flame speed. To understand the reason for the disagreement in predicting the iron effect on the flame speed, we addressed the conclusions of Bolshova and Korobeinichev,⁵ who explained the mechanism of the promotion effect of TMP on low-pressure H₂/O₂/Ar flames. According to ref 5, the catalytic recombination of H and OH radicals results in an increase in the flame temperature and, hence, an increase in the rate of the chain-branching reaction H + O₂ = OH + O. It is claimed in ref 5 that the chain-branching rate determines

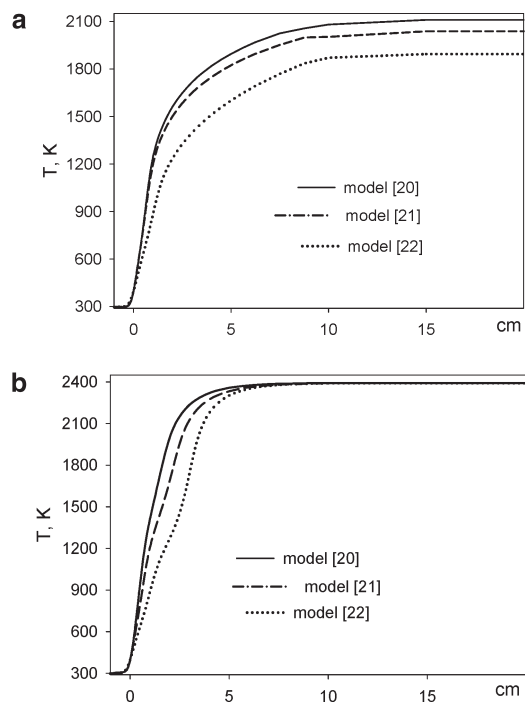


Figure 2. Simulated (using three models^{20–22}) temperature profiles in a H₂/O₂/Ar (0.33762:0.45624:0.20614) flame (a) without additive and (b) with 0.1% atomic iron at $P = 3$ kPa and $T_0 = 298$ K.

Table 1. Calculated Speed and Final Temperature of H₂/O₂/Ar Flame ($\phi = 0.37$; P , 3 kPa; T_0 , 298 K) without Additive and with 0.1% (by Volume) Atomic Iron

mechanism	burning velocity, u (cm/s)			temperature, T_f (K) ^a		
	clear	0.1% Fe	Δu^b	clear	0.1% Fe	ΔT^c
Curran ²⁰	252.4	255.2	+2.8	2110	2392.1	282.1
Dryer ²¹	247.6	240.9	–6.7	2037.1	2389.8	352.7
Konnov ²²	198.8	193.5	–5.3	1893.4	2390.2	496.8

^a Temperature at the right boundary of the computational grid. ^b $\Delta u = u - u_0$. ^c $\Delta T = T_f - T_f^0$.

the increase in the flame speed, despite a decrease in the H and OH radical concentrations.

Panels a (modeling with the mechanism from ref 20) and b (modeling with the mechanism from ref 22) of Figure 3 show the net reaction rate of H + O₂ = OH + O over the flame zone for the undoped flame and that doped with 1000 ppm Fe. A 30% increase in the net reaction rate in the Fe-doped flame is observed in the case of using the mechanism from ref 20 and the mechanism from ref 22 predicts a small decrease in the chain-branching rate in the Fe-doped flame. Sensitivity analysis revealed a high sensitivity of the flame speed to the rate constant of the chain-branching reaction. Therefore, a decrease (increase) in the flame speed is largely determined by the dopant influence on the chain-branching rate.

Therefore, the mechanisms from refs 20 and 22 provide essentially different results, whereas the results obtain with the mechanism from ref 21 lie between them. Therefore, the modeling results obtained with the mechanism from ref 21 were not presented in Figure 3 and hereafter for space-saving reasons.

The inhibition effect observed in using Konnov's mechanism²² is related to the stepped shape of the temperature profile (Figure 2b): the temperature rise in the doped flame (relative to the undoped flame) occurs at 2 cm from the

(25) Turanyi, T.; Zsely, I. G.; Frouzakis, C. KINALC: A CHEMKIN based program for kinetic analysis (available at <http://www.chem.leeds.ac.uk/Combustion/Combustion.html>).

(26) Turanyi, T. MECHMOD, version 1.4: Program for the transformation of kinetic mechanisms (available at <http://www.chem.leeds.ac.uk/Combustion/Combustion.html>).

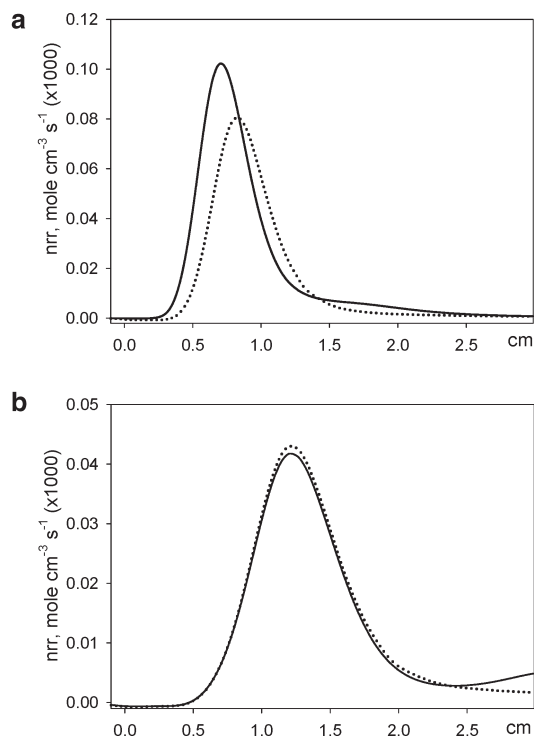


Figure 3. Spatial variation of the net rate of the chain-branching reaction $\text{H} + \text{O}_2 = \text{OH} + \text{O}$ (NRR) in a $\text{H}_2/\text{O}_2/\text{Ar}$ (0.33762:0.45624:0.20614) flame without additive (\cdots) and doped with 0.1% atomic iron (—) at $P = 3$ kPa and $T_0 = 298$ K. Mechanisms from (a) ref 20 and (b) ref 22 were used for modeling.

coordinate origin, where the net rate of chain branching is low. Curran's model²⁰ gives a smooth temperature profile in both the undoped and Fe-doped flames. In this case, the excess of the temperature of the doped flame over that of the undoped flame is observed at 1 cm from the coordinate origin near the maximum of the chain-branching rate, resulting in the promotion of the flame. The effect of atomic iron on the chain-branching rate is demonstrated in panels a (mechanism from ref 20) and b (mechanism from ref 22) of Figure 3. It is noteworthy that the maximum chain-branching rate for the undoped flame predicted by Curran's model²⁰ is 20 times higher than that predicted by Konnov's model.²² This difference between models from refs 20 and 22 may account for the significantly different values of the flame speed predicted by these mechanisms (Table 1).

Spatial variations of the heat release rate in flames without additive and with 1000 ppm Fe (panels a and b of Figure 4) calculated using both mechanisms of H_2 oxidation^{20,22} helped us to determine the flame zone in which the heat was released. The shape of the temperature profile for the Fe-doped flame depends upon the flame region where the heat from the reactions involving ICS is released. The appearance of additional maxima (at higher temperatures) in the temperature profiles of the doped flames (Figure 4b) indicates that the heat release from the reactions involving ICS occurs at higher temperatures than that from hydrogen oxidation. The validity of this conclusion is obviously demonstrated by Figure 5, in which the heat release rates in hydrogen oxidation and in the reactions involving ICS are shown as separate curves (modeling with Konnov's model²²). One can see that these curves do not coincide spatially. The flame regions of the heat release from hydrogen oxidation and from ICS-involving reactions overlap to a greater extent if Curran's mechanism²⁰ is used

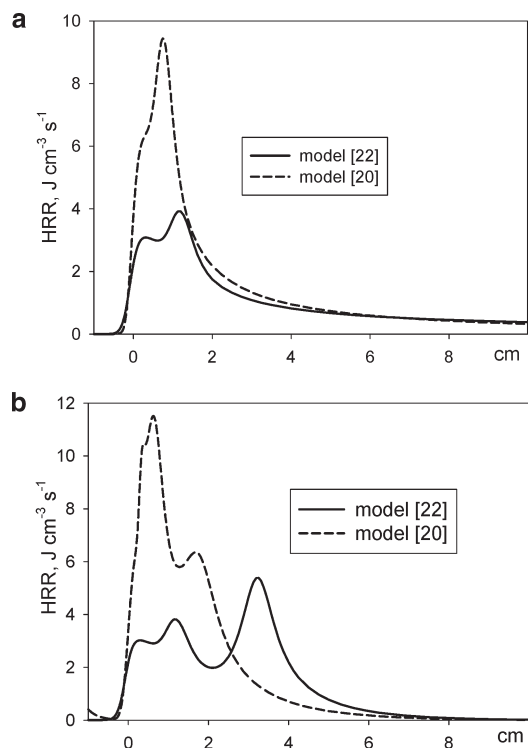


Figure 4. Spatial variation of the heat release rate calculated using the mechanisms from refs 20 and 22 for a $\text{H}_2/\text{O}_2/\text{Ar}$ (0.33762:0.45624:0.20614) flame (a) without additive and (b) doped with 0.1% atomic iron at $P = 3$ kPa and $T_0 = 298$ K.

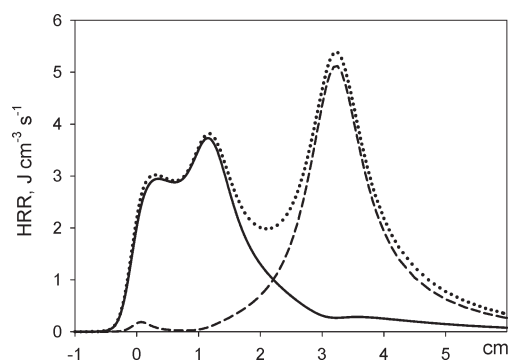


Figure 5. Spatial variation of the heat release rate in hydrogen oxidation (—) and the reactions involving ICS (---) and the total heat release rate (\cdots) in a $\text{H}_2/\text{O}_2/\text{Ar}$ (0.33762:0.45624:0.20614) flame doped with 0.1% atomic iron at $P = 3$ kPa and $T_0 = 298$ K.

and to a lesser extent for mechanism from ref 22. This feature of the H_2 oxidation mechanism determines the influence of the iron additive on the net rate of chain branching and, hence, on the flame speed. In the case of considerable overlap of the flame regions of heat releases from H_2 oxidation and ICS-involving reactions, the additional heat influences the chain-branching rate, thus raising the flame speed. If the flame regions overlap only slightly, the additional heat does not increase the temperature in the flame zone where chain branching occurs and the net rate of the chain-branching reaction does not change. In this situation, the flame speed does not increase and its reduction with respect to that of the undoped flame may be explained by a decrease in the concentrations of H and O atoms (the OH level appreciably increases as the dopant is added).

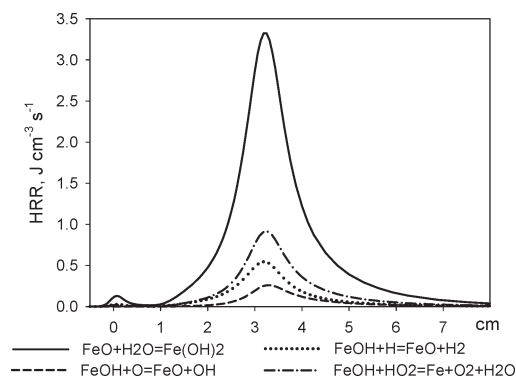


Figure 6. Spatial variation of the heat release rate in separate reactions, involving ICS, in a $\text{H}_2/\text{O}_2/\text{Ar}$ (0.33762:0.45624:0.20614) flame doped with 0.1% atomic iron at $P = 3$ kPa and $T_0 = 298$ K.

It is interesting to compare these results to those obtained by Bonne et al. Bonne et al.²⁷ spectroscopically studied premixed flat CH_4/O_2 and CH_4/air flames doped with $\text{Fe}(\text{CO})_5$ (100 ppm) at a pressure of 8 kPa (about 60 Torr). They found the effect of $\text{Fe}(\text{CO})_5$ on the peak OH mole fraction to be negligible, but the decay rate of the OH radical increased in the $\text{Fe}(\text{CO})_5$ -doped flame quite noticeably. This observation obviously demonstrated that the process of radical recombination, catalyzed by iron species, proceeded downstream in relatively the zone of methane oxidation. This feature is also inherent to the lean flame studied in the present work, where the peak rate of ICS-involving reactions is observed at higher temperatures than hydrogen oxidation.

Thus, the inhibition or promotion effect of atomic iron additive on the flame speed is determined by the mechanism for H_2 oxidation rather than the reactions of ICS.

The reactions involving ICS that make a major contribution to the additional heat release and their heat release rates are given in Figure 6. The reaction of iron hydroxide formation $\text{Fe} + \text{H}_2\text{O} = \text{Fe}(\text{OH})_2$ makes a 60% contribution to the additional heat release. Apparently, an increase in the temperature is due to the recombination of atoms catalyzed by ICS but not the oxidation of the additional fuel (Fe) doped to the flame.

The mechanism of flame promotion by organophosphorus compounds is also related to additional heat release in the reactions involving phosphorus compounds. It is therefore of interest to compare the effect exerted on the same flame by iron and organophosphorus compounds, which were shown to be promoters for low-pressure near-stoichiometric flames. The determination of characteristic features of the iron and phosphorus effects on the flame will allow us to find significant regularities in the effect of the additional heat release on the flame speed. It is also important to elucidate how the choice of the mechanism for hydrogen oxidation^{20,22} influences the predicted promotion effectiveness.

3.2. Effect of Organophosphorus Compounds on the Flame. Although the effect of TMP on the net rates of the chain-branching reaction and the key reaction of catalytic recombination $\text{H} + \text{PO}_2 + \text{M} = \text{HOPO} + \text{M}$ has been studied in great detail,³ the flame region of additional heat release has not been determined and this issue has not been considered. Thus, it was of interest to study this aspect of TMP combustion chemistry.

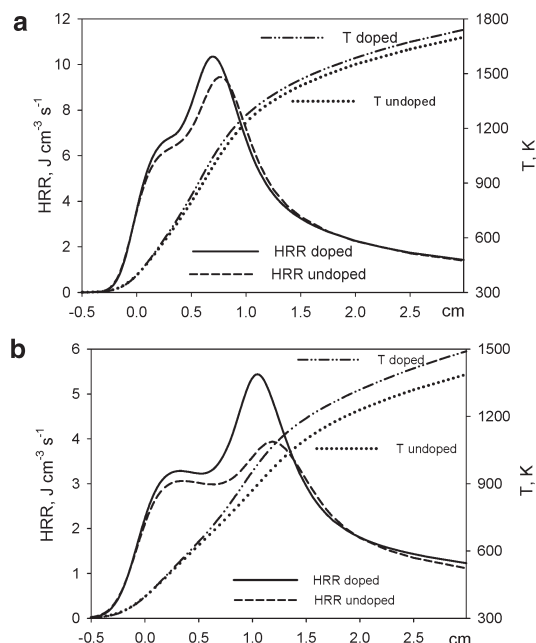


Figure 7. Spatial variation of the heat release rate and temperature in a $\text{H}_2/\text{O}_2/\text{Ar}$ (0.33762:0.45624:0.20614) flame without additive and doped with 0.1% atomic iron at $P = 3$ kPa and $T_0 = 298$ K. Mechanisms from (a) ref 20 and (b) ref 22 were used for modeling.

Our modeling shows that, in the TMP-doped flame, additional heat is released in exactly the same flame region as that from H_2 oxidation, as evidenced by similarity in heat release rate profiles for the undoped and doped flames (panels a and b of Figure 7). This feature of TMP as a flame promoter distinguishes it from iron. The coincidence of the flame regions of heat releases from H_2 oxidation and phosphorus-involving reactions results in a temperature rise throughout the flame zone, which increases the chain-branching rate. That is why TMP promotes the flame. According to modeling calculations using Curran's mechanism,²⁰ the maximum temperature of a TMP-doped flame (1000 ppm) is 184 K lower than the equilibrium value, and for Konnov's model,²² this value is equal to 394 K. Different mechanisms for hydrogen oxidation predict different promotion effectiveness. Thus, Curran's model²⁰ predicts a 0.5% increase in the flame speed, whereas Konnov's model²² predicts a 1.7% increase in the flame speed, which correlates to a greater increase in the heat release rate (and flame temperature). The promotion effect of TMP on the flame is observed despite the lower kinetic thermal effect of TMP than that of iron at equal concentrations.

Therefore, the effect of additives on the flame speed is determined not so much by the amount of heat release but by the flame region where the additional heat is released. A comparison of the effect of iron and TMP on the same flame clearly demonstrates this conclusion.

It should also be noted that the addition of TMP introduces additional fuel to a lean ($\phi = 0.37$) flame, which contributes to the promotion. However, a comparison of the equilibrium temperatures for the undoped and TMP-doped (1000 ppm) mixtures revealed a small difference of 10 K. Thus, the contribution of the additional fuel to promotion does not exceed 5%.

Using sensitivity analysis, it has been found⁵ that the reaction $\text{H} + \text{PO}_2 + \text{M} = \text{HOPO} + \text{M}$ plays a key role in promotion, but no explanation has been proposed. The calculation of the heat release rate in the TMP-doped flame shows that most of

(27) Bonne, U.; Jost, W.; Wagner, H. G. *Fire Res. Abstr. Rev.* **1962**, *4*, 6–18.

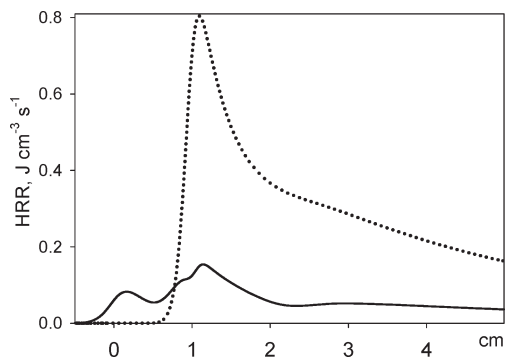


Figure 8. Spatial variation of the heat release rate (HRR) in a $\text{H}_2/\text{O}_2/\text{Ar}$ (0.33762/0.45624/0.20614) flame doped with 0.1% of trimethyl phosphate at $P = 3$ kPa and $T_0 = 298$ K; modeling was performed using mechanism from ref 22; \cdots , HRR in the reaction $\text{H} + \text{PO}_2 + \text{M} = \text{HOPO} + \text{M}$; —, HRR in all reactions involving phosphorus except for that above mentioned.

the additional heat in the reactions involving phosphorus is released in the above reaction (Figure 8), which explains its important role in the promotion effect. Other reactions with the participation of phosphorus compounds give no more than 10% of the additional heat release. In the low-temperature

flame zone, heat is released from the decomposition reaction $(\bullet\text{CH}_2\text{O})(\text{CH}_3\text{O})_2\text{PO} = (\text{CH}_3\text{O})_2\text{PO} + \text{CH}_2\text{O}$.

4. Summary

The promotion and inhibition effect of iron on the flame speed is determined not so much by the amount of heat release but by the flame region where the additional heat is released. The flame region where the additional heat is released, in turn, is determined by the mechanism for hydrogen oxidation, which is also responsible for the inhibition (promotion) effectiveness.

The maximum promotion effectiveness is observed when the flame region of the additional heat release coincides with that of the maximum chain-branching rate.

In the iron-doped flame, the reaction of iron hydroxide formation $\text{FeO} + \text{H}_2\text{O} = (\text{Fe}(\text{OH})_2)$ makes a more than 50% contribution to the additional heat release. In the phosphorus-doped flame, the recombination reaction $\text{H} + \text{PO}_2 + \text{M} = \text{HOPO} + \text{M}$ produces more than 90% of the additional heat.

Acknowledgment. We thank Professor F. Dryer and Professor A. Konnov for providing the kinetic model for hydrogen oxidation and Dr. G. T. Linteris for providing the kinetic model for flame inhibition by iron pentacarbonyl.